Strong interatomic effects accompanying core ionization of atomic clusters

N. V. Dobrodey
Institut für Theoretische Astrophysik, Universität Heidelberg, D-69121 Heidelberg, Germany

A. I. Streltsov and L. S. Cederbaum
Theoretische Chemie, Universität Heidelberg, D-69120 Heidelberg, Germany

(Received 22 February 2001; published 10 January 2002)

Fourth-order Green's function calculations have revealed many interesting features in the core-level spectra of Be_n and Mg_n ($n=2,3,4$) clusters. The most striking of them are unusually low-lying intense satellites. These are absent in the respective atomic spectra and not observed in the spectra of typical molecules. An analysis in terms of localized configurations attributes these satellites to distinct *interatomic* processes. These processes comprise charge and energy transfer from one atom to neighboring atoms. The spectra are sensitive to the size and conformation of the clusters. This can be useful for the experimental identification of the clusters. The emerging physical picture of core ionization of small soft metal Be_n and Mg_n clusters is quite general and applicable to other weekly bound atomic and molecular clusters.

DOI: 10.1103/PhysRevA.65.023203 PACS number(s): 36.40.Cg, 36.40.Mr, 33.60.Fy

I. INTRODUCTION

Atomic and molecular clusters represent a specific class of objects that have their own peculiar properties differing from those of molecules and solids (bulk). Clusters can be also thought of as a natural bridge between atoms (molecules) and solids [1]. Size dependence of different cluster properties and their evolution to properties of the bulk is the subject of most studies in cluster science. Until recently, the majority of cluster studies have been devoted to the properties of the ground electronic state (geometries, dynamics of formation and fragmentation, interatomic and intermolecular potentials, and vibrational excitations) and to low-lying electronic excitations (valence photoabsorption and photoionization) [1–6]. The considerable progress made in the last years in the field of tunable x-ray high-intensity sources, and the developments of new coincidence detection techniques and cluster beam sources with high size selectivity enable one to study highly excited electronic states of clusters.

Core-level spectroscopies (photoelectron, photoabsorption, and Auger) are well suited for studying clusters. Due to a compactness of atomic core levels, core-level spectroscopies basically probe local properties, providing information on the chemical state of selected atomic species. On the other hand, core-level spectroscopies allow one to study also nonlocal processes (interatomic or intermolecular) occurring upon core ionization, core excitation or core-hole Auger decay. These interatomic processes comprise different valence electronic excitations of atoms (molecules) neighboring the atom with the initial core vacancy. As we shall see, these excitations may appear in the spectra as satellites. Of course, there are also satellites in the core-level spectra that correspond to local valence excitations, i.e., to excitations of that atom with the core vacancy. To study the various local and nonlocal excitation processes one should clearly identify the respective features in the spectra. Usually, the interpretation of satellite structures in experimental spectra is quite a tedious task even for simple objects and it can hardly be done without a suitable theoretical support. Among several experimental core-level studies of atomic and molecular clusters, there are only a few x-ray photoelectron investigations available in the literature [7–10]. In these works clusters of rather large size have been investigated. In the present paper we theoretically study the core ionization spectra of small metal clusters.

It is well known that *ab initio* calculations of core-level spectra are rather cumbersome. This is due to the fact that electron relaxation and correlation in the core-ionized (core-excited) states are usually strong. Therefore, the use of advanced many-body approaches that can take a substantial fraction of electron relaxation and correlation into account is required. In practice, high-level *ab initio* calculations on core-hole states can be performed only for relatively small objects consisting of a few atoms. Small atomic and molecular clusters are of course, interesting by themselves. In the present paper we concentrate on weakly bound systems that we consider particularly interesting. Typically, neutral clusters built of elemental units (atoms or molecules) with closed electronic shells, are weakly bound systems. The weakness of the chemical bond favors a strong localization of electron vacancies created upon excitation of the cluster. This localization plays a crucial role in the inner-valence photoionization of weakly bound hydrogen-bonded [11,12] and van der Waals [13] clusters, providing a basic condition for the ultrafast decay of the inner-valence vacancy via the so-called *intermolecular Coulombic decay* mechanism [11]. We would like to stress that the effects we would like to study are present already in very small clusters, where the calculations and the analysis of these effects is much easier to perform unambiguously.

To study cluster-specific effects in the core ionization, we have chosen clusters of soft metal atoms (Be and Mg). This choice is governed by the fact that small Be_n and Mg_n clusters ($n=2-4$) are, first of all, weakly bound (see, for example, Ref. [14]) and, in addition, their relatively small size allowed us to calculate the spectra of core ionization at a high level of theory. Moreover, the interatomic distances and bonding properties of these clusters are very sensitive to the

cluster size [14]. This prompts us to expect that the spectral bandshapes should also depend sensitively on the cluster size and conformation.

II. THEORETICAL BACKGROUND AND DETAILS OF THE CALCULATIONS

A. The spectrum

The chemical bond in the ground state (GS) of small Be and Mg clusters is rather weak and interatomic distances are large. For example, the experimental binding energies of Be_2 and Mg_2 are 0.098 [15] and 0.050 eV [16], and the interatomic distances are 4.63 [15] and 7.35 a.u. [16], respectively. In such cases the use of size-consistent methods to compute the electronic structure is imperative. We used the *ab initio* one-particle Green's function (GF) method within the algebraic diagrammatic construction (ADC) scheme consistent through fourth order in the Coulomb interaction [GF ADC(4)] [17,18] to compute core-ionization spectra. Apart from being complete up to fourth order, the ADC(4) method includes partial summations of diagrams to infinite order. What is particularly important in our study is that the method is size consistent, i.e., the results scale correctly with the size of the system [17].

The ionization energies and intensities of lines in the core-ionization spectrum appear in the spectral representation of the Green's function as the pole positions and their residues, respectively. In more exact terms, the residues enter the definition of the intensities I_n within the sudden ionization approximation [19]

$$I_n \sim \left| \sum_c \tau_c x_c^{(n)} \right|^2, \tag{1}$$

where n specifies the core-ionized state, τ_c is the photoionization amplitude of the core orbital c, and the summation is over all core orbitals of the same symmetry. The spectroscopic amplitudes $x_c^{(n)}$ are defined as

$$x_c^{(n)} = \langle \Psi_n^{N-1} | \hat{a}_c | \Psi_0^N \rangle, \tag{2}$$

where Ψ_0^N and Ψ_n^{N-1} denote the exact GS of the N-electron system (neutral) and the exact nth state of the $N-1$ electron system (ionized); $\hat{a}_c$ is the annihilation operator for the core electron in the level c. In most cases the core electron can be localized in space and then only one core orbital contributes to the intensities I_n,

$$I_n \sim |\tau_c|^2 |x_c^{(n)}|^2, \tag{3}$$

$\chi_c^{(n)} = |x_c^{(n)}|^2$ is called spectroscopic factor. For that core-ionized spectrum $\Sigma_n \chi_c^{(n)} = 1$. When the ionizing photon is of high energy, $|\tau_c|^2$ is essentially a constant and the relative intensity of two lines in the spectrum is just given by the quotient of the respective spectroscopic factors.

The meaning of the spectroscopic amplitude $x_c^{(n)}$ is clear from its definition [Eq. (2)]. The sudden removal of a core Hartree-Fock (HF) particle from the exact GS $|\Psi_0^N\rangle$ leads to $\hat{a}_c|\Psi_0^N\rangle$ that is not an eigenstate of the ion. Thus, $x_c^{(n)}$ is the amplitude of probability to find the exact eigenstate $|\Psi_n^{N-1}\rangle$ of the ion in $\hat{a}_c|\Psi_0^N\rangle$. In those cases where the ground state of the system is not strongly correlated, i.e., well described by a single determinant, and, in addition, electron relaxation and correlation are not strong in the final core-ionized states, the lowest-energy line in the spectrum is the most intense one. This line is referred to as the *main line*. The corresponding state can be crudely described by a single determinant with a single electron removed from the core. Other lines in the spectrum in this case have low intensity and correspond to different excitations of the above electronic configuration with the core hole. These lines are referred to as *satellites* (shake up and shake off). Under the above-mentioned conditions the spectroscopic factor $\chi_c^{(n)}$ of the main line is typically about 0.8. This means that the remaining spectral intensity (20%) is borrowed by the satellites. In those cases where many-electron effects are stronger, the main line will have a smaller spectroscopic factor. In some specific unusual cases the main line is not necessarily the lowest-energy line in the spectrum. Satellites below the main line may appear, which are referred to as *shake-down* satellites. For example, the lowest-energy lines in the N $1s^{-1}$ spectrum of paranitroaniline [20] and of the metal/adsorbate N_2/Ni(100) system [21] are shake-down satellites.

The configuration space in the ADC(4) scheme comprises all singly and doubly excited configurations of the ground-state HF determinant with an additional electron removed from the core. In other words, the configuration space comprises all $2h1p$ and $3h2p$ configurations (h denotes hole, p denotes particle) with respect to the HF ground-state determinant, where one of the holes is from the core. The method requires as input data the HF orbitals and their energies. They have been calculated using the US GAMESS codes [22] in the 6-311g* atomic basis [23]. The choice of this basis is governed by the fact that our ADC(4) calculations on the Be $1s^{-1}$, Mg $1s^{-1}$, and Mg $2s^{-1}$ core-ionized states of the Be and Mg atoms reproduce the experimental ionization energies for the main lines and shake-up satellites quite well (see Sec. III A) despite the moderate size of the basis set. The relatively small size of the atomic basis set allowed us to perform GF ADC(4) calculations on the clusters consisting of up to four atoms. Although larger basis sets can be used for the smaller clusters, we have decided to discuss all spectra on the same level.

For the Mg_3 and Mg_4 clusters studied here the GF ADC(4) configuration space becomes large. To make possible calculations on the core-ionized states of these clusters we had to freeze the $1s$ and $2p$ core electrons in the clusters. We have checked for the smaller systems that for ionization of the Mg $2s$ level the freezing of Mg $1s$ and Mg $2p$ electrons does not lead to a significant change of the absolute ionization energies.

B. Conformations and interatomic distances of the clusters

For the sake of consistency the equilibrium interatomic distances for the Be_n and Mg_n clusters have been obtained with the above-mentioned basis set at the level of the fourth-

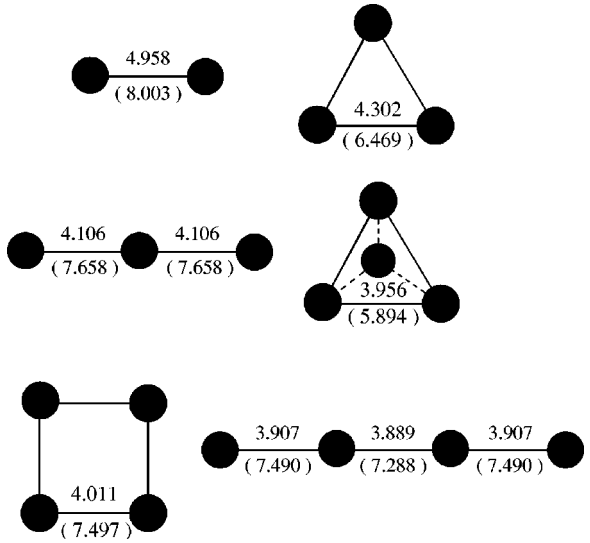

FIG. 1. The computed geometries of the Be_n and Mg_n clusters. The interatomic distances (a.u.) for Mg_n clusters are shown in parentheses.

order Møller-Plesset perturbation theory (MP4) using the GAUSSIAN98 codes [24]. The computed geometries are depicted in Fig. 1.

Experimental data on the geometries of the clusters are only available for the dimers [15,16]. Computational data on Be and Mg clusters have been amply reported in the literature (see Ref. [25] and references therein).

Our computed interatomic distances for the Be_3 triangular and Be_4 tetrahedral clusters are consistent with the MP4 results obtained in the larger 6-311+g* basis set [26]. For the Mg_3 triangular and Mg_4 tetrahedral clusters our MP4 distances are close to the results of multireference configuration interaction calculations available in the literature obtained using similar or better quality basis sets [27].

The MP4 GS interatomic distances obtained in the 6-311g* basis set for the Be and Mg dimers are satisfactorily close to those derived from experiment. The Be-Be MP4 equilibrium distance is 4.958 a.u., whereas the respective experimental value is 4.63 a.u. [15]. For Mg_2 the experimental Mg-Mg distance is 7.35 a.u. [16]. MP4 gives for this value 8.003 a.u. To avoid a misunderstanding, we should note that calculations on the ground-state properties of Be_2 and Mg_2 represent a rather delicate problem. The equilibrium distances and binding energies of these dimers are very sensitive to the atomic basis set and to the method used to account for electron correlation (see, for example, Refs. [28,29]). The results obtained in the 6-311g* basis set at the MP4 level can be thought of as a good compromise between the size of the atomic basis set and the accuracy of the computed GS properties.

III. RESULTS

A. Be and Mg atoms

We begin with the core-level spectra of the elemental units of our Be and Mg clusters, i.e., of the Be and Mg neutral atoms. The atomic spectra are of interest owing to several reasons. First, one should be able to distinguish between local (atomic) and nonlocal (interatomic) effects in the spectra of the clusters. It is also of interest to study the evolution of the spectral band shapes from atoms to clusters. Second, the atomic core-level spectra are of interest by themselves. Indeed, for the Mg atom the experimental data are available only for the main lines (Mg $1s^{-1}$, Mg $2s^{-1}$) [30,31]. The satellite structures in the core ionization spectra of the atomic Mg are poorly understood. Third, the experimental data available for the ionization energies of the main $1s^{-1}$ line and shake-up satellites of atomic Be [32] allows us to estimate the reliability of our ADC(4) calculations on the spectra.

The agreement between our computed ionization energies in the Be $1s^{-1}$ spectrum and experimental ones [32] is more than satisfactory (Table I). For the Be atom full configuration interaction (CI) calculations have been reported in the literature [33]. The quality of the basis set used in these calculations is comparable to that used in our work. As anticipated,

TABLE I. GF ADC(4) absolute (E_i) and relative (ΔE_i) energies and intensities ($\chi_c^{(i)}$) of lines in the Be $1s^{-1}$ ionization spectrum of the Be atom in comparison with the available experimental and theoretical data. All energies in eV.

Theory —GF ADC(4)—			—Full CI[b]—			Experiment[a]		
E_i	ΔE_i	$\chi_c^{(i)}$	E	ΔE_i	$\chi_c^{(i)}$	E	ΔE_i	State characterization
123.33	0.0	0.717	123.62	0.0	0.77	123.6	0.0	$1s2s^2\,(^2S)$
127.82	4.49	0.0	128.37	4.75	0.0	128.0	4.4	$1s2s2p\,(^2P)$
130.12	6.79	0.0	131.32	7.7	0.0	130.2	6.6	$1s2s2p\,(^2P)$
131.02	7.69	0.0				131.7	8.1	$1s2p^2\,(^2D)$
133.05	9.72	0.094	136.07	12.45	0.017	135.1	11.5	$1s2p^2\,(^2S)$
138.32	14.99	0.059	138.77	15.15	0.1	138.1	14.5	$1s2s3s\,(^2S)$
138.32	14.99	0.0	139.09	15.47	0.0	138.7	15.1	$1s2s3p\,(^2P)$
140.79	17.46	0.079	140.69	17.07	0.075	140.5	16.9	$1s2s3s\,(^2S)$

[a]Reference [32].
[b]Reference [33].

TABLE II. GF ADC(4) absolute (E_i) and relative (ΔE_i) energies and intensities ($\chi_c^{(i)}$) of lines in the Mg $2s^{-1}$ ionization spectrum of the Mg atom in comparison with the available theoretical data. The experimental ionization energy for the Mg $2s^{-1}$ main line is 96.5 eV [31]. All energies in eV.

Theory						
—GF ADC(4)—			—Limited CI[a]—			
E_i	ΔE_i	$\chi_c^{(i)}$	E_i	ΔE_i	$\chi_c^{(i)}$	State characterization
97.45	0.0	0.787	96.85	0.0	0.760	Mg $2s^{-1}$ (^2S)
101.78	4.33	0.0	102.03	5.18	0.0	$2s3s3p$ (^2P)
104.10	6.65	0.0	105.18	8.33	0.0	$2s3s3p$(^2P)
107.79	10.34	0.0	109.23	12.38	0.0	$2s3s3d$ (^2D)
107.84	10.39	0.091	107.97	11.12	0.175	$2s3s4s$ (^2S)
108.77	11.32	0.062	108.28	11.43	0.002	$2s3s4s$ (^2S)
			109.73	12.88	0.09	$2s3s4s$ (^2S)
109.21	11.76	0.0				$2s3p^2$,$2s3p4p$ (^2P)
109.33	11.88	0.0				$2s3p^2$,$2s3p4p$ (^2P)
110.60	13.15	0.0				$2s3p^2$,$2s3p4p$ (^2P)
110.80	13.35	0.0	111.81	14.96	0.0	$2s3s3d$ (^2D)
111.03	13.58	0.014				$2s3p4p$ (^2S)

[a]Reference [33].

we see that the quality of our GF ADC(4) results on the main and singly excited states is close to that of the full CI (Table I).

The experimental and theoretical data available on the ionization of the core levels of atomic Mg are very limited. The GF ADC(4) ionization energy for the Mg $1s^{-1}$ main line (1309.98 eV) is quite close to the experimental value of 1311.5 eV reported in Ref. [30]. For the ionization of the Mg $2s$ level the agreement between our theoretical value for the energy of the main line (97.45 eV) and the experimental one (96.5 eV [31]) is also satisfactory. We list our computed ionization energies for the Mg $2s^{-1}$ spectra together with the available literature data in Table II. Comparing our ADC(4) results with those obtained with the CI method [33] in the basis of comparable quality one can see that the energies of some satellite states relative to the main line differ in these two calculations by ~2 eV. Here we should note that the CI used in Ref. [33] for the calculation of the Mg $2s^{-1}$ ionized states is a limited CI and not a full one.

It is interesting to compare the Be and Mg core ionization spectra. The first two satellites ($2h1p$) in the Be $1s^{-1}$ spectrum appear at 4.5 and 6.8 eV above the main line and do not acquire any intensity (Table I). This is because the symmetry of these satellite states is P and thus they cannot couple to the Be $1s^{-1}$ single-hole state that has S symmetry. The first $3h2p$ satellite in the spectrum is at 7.7 eV. Because of its D symmetry this satellite is also dark in the spectrum. In the Mg $2s^{-1}$ spectrum (Table II) the first two satellites are dark because of their P symmetry and their energies relative to the main line (4.3 and 6.6 eV) are very close to those of the first two satellites in the spectrum of Be. The $3h2p$ satellites in the spectrum of Be lie significantly lower in energy than those in the spectrum of Mg. The first bright satellite, which is rather intense, appears at 9.7 and 10.4 eV in the Be $1s^{-1}$ and Mg $2s^{-1}$ spectra, respectively.

Summarizing, both the Be $1s^{-1}$ and Mg $2s^{-1}$ spectra of atomic Be and Mg do not exhibit any visible satellites at energies below about 10 eV.

B. Be_2 and Mg_2 clusters

The most striking features in the computed Be $1s^{-1}$ and Mg $2s^{-1}$ spectra of Be_2 and Mg_2 are intense low-lying satellites in the energy region below 10 eV above the main lines (Figs. 2 and 3). The spectroscopic factors for the main lines in the Be $1s^{-1}$ and Mg $2s^{-1}$ spectra are 0.442 and 0.653 (Tables III and IV), respectively. This means that a large fraction, namely, 66% of the total spectral intensity in the Be $1s^{-1}$ spectrum is borrowed by satellites. In the spectrum of Mg_2 the intensity borrowed by satellites is much smaller (35%). In the Be $1s^{-1}$ and Mg $2s^{-1}$ spectra of the Be and Mg atoms the spectroscopic factors of the main lines were seen in the preceding subsection to be considerably larger ($\chi_c = 0.717$ and 0.787, respectively) than those in the spectra of the respective dimers. Thus, despite the rather weak chemical bonding in Be_2 and Mg_2, electron correlation in the final core-ionized states is much stronger, especially for Be_2, than in the respective atoms.

The first satellites appear in the Be $1s^{-1}$ and Mg $2s^{-1}$ spectra at the surprisingly low energies of 1.68 and 1.32 eV, respectively (Tables III and IV). These satellites are mostly due to valence excitations of electrons from occupied orbitals built of Be $2s$ (Mg $3s$) atomic orbitals to the unoccupied orbitals built of Be $2p$ (Mg $3p$) atomic orbitals. The satellites are characterized by intermediate triplet spin coupling of these valence excitations and their spectroscopic factors $\chi_c = 0.033$ and 0.001 predict lines of moderate and weak intensity in the Be $1s^{-1}$ and Mg $2s^{-1}$ spectra, respectively. The corresponding intermediate singlet counterparts of these satellites are at 4.47 and 2.27 eV in the Be $1s^{-1}$ and Mg $2s^{-1}$ spectra, respectively, and predicted to be remarkably

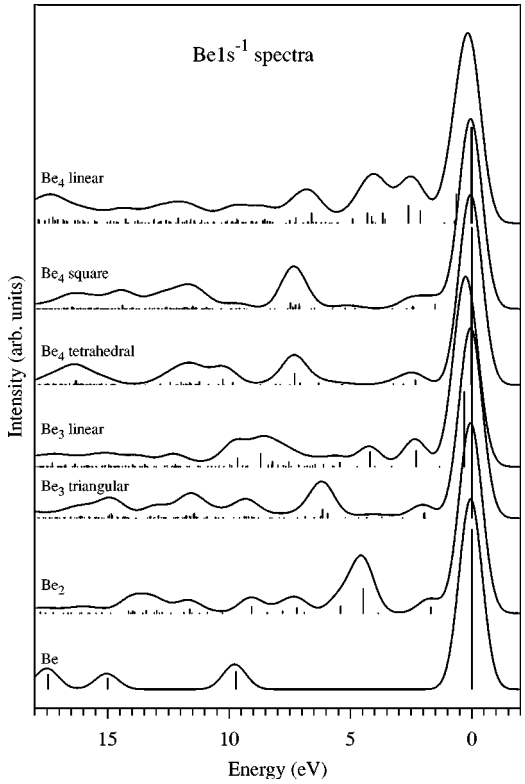

FIG. 2. The computed $1s^{-1}$ ionization spectra of atomic Be and small Be clusters. The spectra were aligned with respect to the lowest-energy lines. The vertical lines represent the energies and intensities (spectroscopic factors) of the final states in the spectrum.

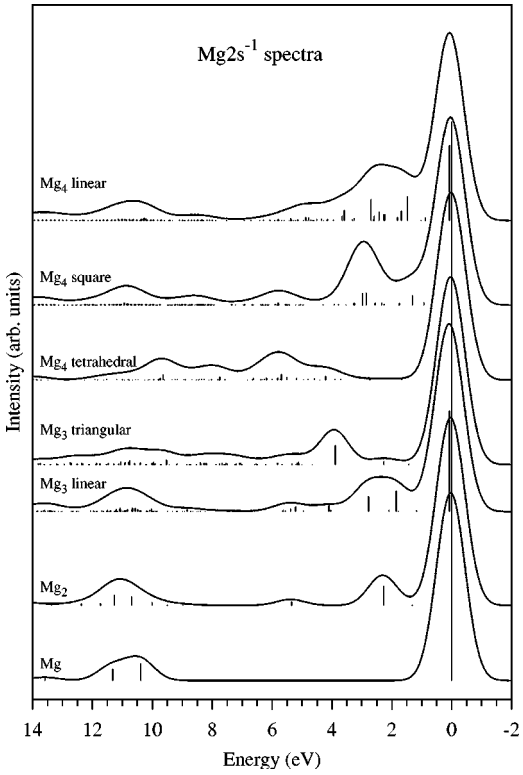

FIG. 3. The computed $2s^{-1}$ ionization spectra of atomic Mg and small Mg clusters. The spectra were aligned with respect to the lowest-energy lines. The vertical lines represent the energies and intensities (spectroscopic factors) of the final states in the spectrum.

intense ($\chi_c = 0.128$ and 0.105). All these satellites are dominated by $2h1p$ configurations.

In contrast to the Mg $2s^{-1}$ spectrum where low-lying doubly excited core-hole states are absent, the Be $1s^{-1}$ spectrum reveals satellites at 3.85 and 5.4 eV that are essentially $3h2p$ states in character (Table III). The satellite at 3.85 eV is very weak ($\chi_c = 0.001$) whereas the satellite at 5.4 eV acquires a considerable intensity ($\chi_c = 0.037$). The higher-lying satellites in the Be $1s^{-1}$ spectrum of Be_2 are characterized by a strong mixing of $2h1p$ and $3h2p$ configurations (Table III). In particular, they form intense structures at 7–9 and 11–14 eV above the main line. In the spectrum of Mg_2 the only relatively intense feature in the energy region from 3 to 9 eV is the satellite at 5.35 eV which is essentially a singly excited core-hole state (Table IV). The spectrum of Mg_2 at 10–12 eV resembles the respective spectrum of the atomic Mg (Fig. 3). This structure in the atomic spectrum is almost entirely due to the two $2s3s4s$ shake-up satellites (triplet and singlet intermediate couplings). In the spectrum of Mg_2 the feature that corresponds to the atomic peak consists, however, of 16 low-intensity lines. These lines are Mg $2s^{-1}$ ionized states that are no more dominated by single excitations as those in the atomic case but are strong mixtures of singly and doubly excited configurations (Table IV). Consequently, the structure at 10–12 eV in the spectrum of Mg_2 can be viewed to correspond to the intra-atomic $2s3s4s$ shake-up that is broken down due to its interaction with a dense manifold of double excitations of the dimer. This effect is analogous to the breakdown of the local shake-up found recently in the core-ionization spectra of metal/adsorbate systems [34].

Structures in the spectrum of Be_2 related to intra-atomic shake-up satellites are also seen at 7, 9, 11, and 14 eV (Fig. 2). These intra-atomic satellites are also broken down due their interaction with numerous double excitations similarly to the situation discussed above for Mg_2.

While the intra-atomic shake-up features in the spectra of Be_2 and Mg_2 are rather expected, the appearance of the intense satellites at energies <5 eV is very surprising. Indeed, because of the weak interaction between the atoms of the clusters (the Be and Mg clusters have been shown to be to a great extent van der Waals systems [25]) one would expect that the cluster spectra resemble the spectra of the respective atoms with, maybe, some weak features due to the presence of the neighboring atom. Evidently, an analysis in terms of excitations of gerade (g) and ungerade (u) molecular orbitals ($D_{\infty h}$ symmetry in the case of Be_2 and Mg_2) brings no clarity in the interpretation of the low-lying satellites. This is because the molecular orbitals of the Be_2 and Mg_2 clusters are delocalized between the two atomic centers due to the high symmetry. Therefore, when using these molecular orbitals one cannot separate between processes occurring locally on the same center as the core hole (intra-atomic processes) and those involving excitations of the neighboring atom (interatomic processes).

TABLE III. GF ADC(4) absolute (E_i) and relative (ΔE_i) energies and intensities ($\chi_c^{(i)}$) of lines in the Be $1s^{-1}$ ionization spectrum of the Be_2 cluster. All energies in eV. Only nondegenerate states (splitting $\geqslant$0.001 eV) are listed.

E_i	ΔE_i	$\chi_c^{(i)}$	State characterization (%) $1h/2h1p/3h2p$	State interpretation
121.25	0.0	0.442	44/44/12	Main state
122.93	1.68	0.033	3/76/21	CTS, ET
125.10	3.85	0.001	0/19/81	
125.72	4.47	0.128	13/62/25	CTS, ET
126.65	5.4	0.037	4/4/92	
127.27	6.02	0.0001	0/45/55	Intra-atomic shake up, ET
128.16	6.91	0.005	0/53/47	ET, CTS
128.28	7.03	0.0001	0/28/72	
128.46	7.21	0.029	3/11/86	
129.05	7.8	0.011	1/8/91	
129.68	8.43	0.003	0/42/58	Intra-atomic shake up
130.33	9.08	0.035	4/33/63	

At the self-consistent field (SCF) level the orbitals of the cluster largely keep their atomiclike character. This is reflected in the computed small splitting between the levels of g and u symmetries. This fact allows us to uniquely transform the wave functions from the symmetry adapted to the localized representation. In this way we can separate in each wave function of the core-ionized cluster the contributions of intra-atomic and interatomic processes. This issue is addressed in the following subsection.

C. The localized representation of the core-ionization of Be_2 and Mg_2

The surprisingly low-lying satellites discussed in the preceding subsection are dominated by singly excited configurations that can be expressed in terms of annihilation $\hat{a}$ and creation $\hat{a}^+$ operators as $\hat{a}_{c(g,u)}\hat{a}_{v(g,u)}\hat{a}^+_{v^*(g,u)}|\Psi_0\rangle$, where v, v^*, and c denote valence, virtual, and core orbitals of g and u symmetries, respectively, and $|\Psi_0\rangle$ is the GS wave function. Assuming that the interatomic interaction is negligible, $\hat{a}_{(g,u)}$ can be expressed as follows: $\hat{a}_{(g,u)}=1/\sqrt{2}(\hat{a}_l \pm \hat{a}_r)$, where $+$ and $-$ are for the g and u symmetries, respectively, and l and r denote the ''left'' and ''right'' atomic sites. Each singly excited configuration can now be expressed in terms of the local $\hat{a}_{l,r}$ and $\hat{a}^+_{l,r}$ operators. This *localized* representation allows one to discuss the structure of the core-ionized states in terms of four basic types of configurations: $l^s(ll) \pm r^s(rr)$, $l^s(rl) \pm r^s(lr)$, $l^s(lr) \pm r^s(rl)$ and $l^s(rr) \pm r^s(ll)$. In the following we will use these notations for the excited configurations $c^s(vv^*)$ where c is the core hole on a specific atomic site (left or right) and v and v^* denote the valence $v \rightarrow v^*$ excitation of an electron from one specific site to another. s denotes the intermediate spin of the valence $v \rightarrow v^*$ excitation. For example, $l^s(rl)$ means a core hole on the left atom accompanied by the valence excitation $r \rightarrow l$ from the right to the left atom.

The satellites at 1.68 and 4.47 eV in the Be $1s^{-1}$ spectrum of Be_2 are found to be strong mixtures of the $l^3(rl)$ and $l^3(rr)$, and $l^1(rl)$ and $l^1(rr)$ configurations, respectively. From here on we will omit the full linear combination introduced above indicating g or u symmetry since the meaning is evident. In the Mg $2s^{-1}$ spectrum of Mg_2 the satellites at 1.32 and 2.27 eV are dominated by the $l^3(rl)$ and $l^1(rl)$ configurations, respectively, and the satellites at 3.77 and 5.35 eV correspond mainly to the $l^3(rr)$ and $l^1(rr)$ configurations, respectively. We may conclude that the intense low-lying satellites in the spectra of Be_2 and Mg_2 are due to

TABLE IV. GF ADC(4) absolute (E_i) and relative energies (ΔE_i) and intensities ($x_c^{(i)}$) of lines in the Mg $2s^{-1}$ ionization spectrum of the Mg_2 cluster. All energies in eV. Only nondegenerate states (splitting $\geqslant$0.001 eV) are listed.

E_i	ΔE_i	$\chi_c^{(i)}$	State characterization (%) $1h/2h1p/3h2p$	State interpretation
96.94	0.0	0.653	65/30/5	Main state
98.26	1.32	0.001	0/87/13	CTS
99.21	2.27	0.105	10/78/12	CTS
100.71	3.77	0.0002	0/85/15	ET
101.78	4.84	0.0003	0/86/14	Intra-atomic shake-up
102.29	5.35	0.021	2/79/19	ET

TABLE V. The GF ADC(4) relative energies (ΔE_i) and intensities ($\chi_c^{(i)}$) of the first low-lying satellites in the Be $1s^{-1}$ spectra of the $Be_n(n=3,4)$ clusters. All energies in eV.

Be_3 triangular		Be_4 tetrahedral		Be_4 square	
ΔE_i	$\chi_c^{(i)}$	ΔE_i	$\chi_c^{(i)}$	ΔE_i	$\chi_c^{(i)}$
1.40	3×10^{-6}	2.29	0.025	1.50	0.024
1.93	0.004	2.79	0.007	2.39	0.011
1.95	0.030			2.43	0.011
1.97	0.026				

TABLE VI. The GF ADC(4) relative energies (ΔE_i) and intensities ($\chi_c^{(i)}$) of the first low-lying satellites in the Mg $2s^{-1}$ spectra of the $Mg_n(n=3,4)$ clusters. All energies in eV.

Mg_3 triangular		Mg_4 tetrahedral		Mg_4 square	
ΔE_i	$\chi_c^{(i)}$	ΔE_i	$\chi_c^{(i)}$	ΔE_i	$\chi_c^{(i)}$
1.43	0.004	1.67	0.004	0.92	0.014
2.26	0.017	2.73	0.003	1.300	0.051
				1.305	0.009
				1.75	0.005

nonlocal (interatomic) processes.

Despite the fact that the spectra of the atoms do not exhibit any visible satellites in the energy region from the main line up to ~10 eV, there are low-lying atomic shake-up states that are dark in the spectra (see Sec. III A). In the spectra of the Be_2 and Mg_2 clusters the satellites corresponding to the dark atomic ones may become visible due to symmetry lowering in the cluster. The interaction between the atoms in the cluster is, however, so weak that the satellites originating from these atomic shake-up states remain almost invisible also in the spectra of the clusters (Tables III and IV). Interestingly, these atomiclike satellites are located at much higher energies than are the purely interatomic features discussed above.

D. Triangular, tetrahedral, and square conformers

At first sight the spectra of the triangular Be_3 and the square and tetrahedral conformers of Be_4 to some extent resemble the respective spectrum of the dimer (Fig. 2). The positions of the intense features at low energies are, however, gradually shifted to higher binding energies compared to the spectrum of Be_2 when increasing the cluster size. Interestingly, the interatomic distances in the Be_4 square and tetrahedral conformers are very close to each other (4.011 and 3.956 a.u., respectively) and the positions of the intense low-lying satellites are close in the respective spectra as well (Fig. 2). For the Mg clusters the situation is different: the spectra of the various clusters exhibit a different appearance. In the case of the Mg_4 clusters the interatomic distance of the tetrahedral conformer (5.894 a.u.) differs considerably from that of the square one (7.497 a.u.) and the band shapes of the respective spectra at energies below 6 eV also are very different (Fig. 3). All the spectra of the regular Be_3, Be_4, and Mg_3, Mg_4 clusters exhibit very low lying satellites (Tables V and VI). Most of these satellites are weak. The pattern of those low-lying satellites depends on the geometry of the cluster.

The ionization energies of the main lines in the Be $1s^{-1}$ and Mg $2s^{-1}$ spectra of the Be_n and Mg_n clusters decrease when the cluster size is increasing (Tables VII and VIII). In the sequence Be-Be_2-Be_3 (triangular)-Be_4 (tetrahedral) the ionization energies are 123.33, 121.25, 119.96, 119.00 eV, respectively. One can see that the major change occurs when going from Be to Be_2 (2.08 eV). The difference between the ionization energies of the Be atom and the tetrahedral conformer of Be_4 is 4.33 eV. For the Mg clusters the changes in the ionization energies when increasing the cluster size are less pronounced than for the Be clusters (Table VIII). The ionization energy of the Mg atom is larger than that of the Mg_4 tetrahedral cluster by only 1.48 eV. Interestingly, in the Be $1s^{-1}$ spectra the spectroscopic factor of the main line decreases dramatically from $\chi_c=0.717$ to $\chi_c=0.442$ when going from atomic Be to its dimer Be_2, but from then on this value changes only marginally. It is $\chi_c=0.441$ and $\chi_c=0.469$ for the main lines of the triangular Be_3 and tetrahedral Be_4 clusters, respectively. The situation is different for the Mg clusters. Here, the spectroscopic factor decreases continuously when going from the Mg atom ($\chi_c=0.705$) to Mg_2 ($\chi_c=0.638$) and then to the triangular Mg_3 ($\chi_c=0.512$) to approximately stabilize when arriving at the tetrahedral Mg_4 ($\chi_c=0.551$).

E. Linear Be_3, Be_4 and Mg_3, Mg_4 clusters

In contrast to the regular clusters where all the atoms are geometrically equivalent, the linear Be_3, Be_4 and Mg_3, Mg_4 clusters contain inequivalent atoms. This inequivalence immediately results in some features in the spectra that can be attributed to the ionization of the geometrically different atoms. In the Be $1s^{-1}$ spectrum of the linear Be_3 cluster the main line is split into two components separated by 0.31 eV. The lowest-energy component is due to the ionization of the central Be atom and the second component is related to the ionization of the two terminal atoms. For the lowest-energy state the spectroscopic factor χ_c is 0.454 whereas for the state, corresponding to the ionization of the terminal atoms, χ_c is 0.396 (Table VII). We attribute the smaller value of χ_c in the latter case to the fact that the ionization of the terminal atoms in the Be_3 cluster is accompanied by a charge transfer to the central atom (antiscreening). There are two terminal atoms in linear Be_3 and Mg_3 and, therefore, all lines appearing in the spectrum due to their ionization should be attributed twice the intensity. This is taken into account in the envelope of the spectrum shown in Figs. 2 and 3.

For linear Be_3 there are two low-lying weak satellites at 1.33 and 1.81 eV above the lowest-energy main state, which correspond to the ionization spectra of the terminal ($\chi_c=0.002$) and central ($\chi_c=2\times10^{-5}$) atoms, respectively. Two intense satellites appear at 2.29 and 4.18 eV, which correspond to the ionization spectra of the terminal ($\chi_c=0.085$) and central ($\chi_c=0.118$) Be atoms, respectively.

TABLE VII. Orbital energies (ε_i), GF ADC(4) ionization energies (E_i) and intensities ($\chi_c^{(i)}$) of the main lines in the Be $1s^{-1}$ spectra of atomic Be and Be_n clusters. All energies in eV. Only nondegenerate states (splitting $\geqslant$0.001 eV) are listed.

Cluster	$-\varepsilon_i$	E_i	$\chi_c(i)$	Comments
Bc	128.75	123.33	0.717	
Be_2	128.73	121.25	0.442	
Be_3 triangular	128.46	119.96	0.441	
Be_3 linear	128.33	119.38	0.454	Central atom
	128.44	119.69	0.396	Terminal atoms
Be_4 tetrahedral	127.72	119.00	0.469	
	127.70	118.99	0.471	
Be_4 square	128.53	119.36	0.426	
	128.52	119.35	0.428	
Be_4 linear	127.59	118.14	0.504	Internal atoms
	128.16	118.76	0.155	Terminal atoms

In the case of the linear Be_4 cluster the effects resulting from the inequivalency of the atoms are more pronounced than in the case of the Be_3 cluster (Fig. 2). The first two states in the spectrum of the linear Be_4 cluster are split by 0.61 eV due to the inequivalent amount of many-body effects affecting the pair of internal and the pair of terminal atoms. The lowest-energy line in the spectrum corresponds to the ionization of the internal atoms and the second line is due to the ionization of the terminal ones. The spectroscopic factor of the first line is 0.504 whereas that of the second line is only 0.155. This means that ~85% of the total spectral intensity in the ionization spectrum of the terminal atoms is borrowed by satellites. There is, therefore, a complete breakdown of the quasiparticle picture of the core ionization of the terminal Be atoms in this linear cluster. The main physical mechanism responsible for this breakdown is a strong charge transfer from the internal to the external atoms, which screens the core hole created upon ionization of the terminal Be atoms. In the ground state of the cluster the internal atoms are negatively charged and the creation of a core hole on a terminal atom favors this charge transfer.

There are two very low lying satellites in the Be $1s^{-1}$ spectrum of the Be_4 linear cluster at 0.66 and 1.10 eV above the lowest-energy main line. The spectroscopic factors of these satellites are 0.014 and 0.002, respectively. These satellites are due to the ionization of the internal atoms. The two satellites at 2.08 and 2.58 eV are rather intense ($\chi_c=0.066$ and 0.094, respectively) and they correspond to the ionization spectra of the terminal and internal atoms, respectively.

In the spectra of the linear Mg_3 and Mg_4 clusters the effects due to the inequivalence of the atoms are also present, but not as strongly pronounced as in the spectra of Be_3 and Be_4. The two main states in the spectrum of the Mg_3 linear cluster are split by only 0.08 eV (Table VIII). Their spectroscopic factors are 0.599 and 0.536, respectively. Similarly to Be_n, the lowest-energy state corresponds to the ionization of the central Mg atom and the second state is due to the ionization of the terminal ones. The two low-lying satellites at 1.17 and 1.78 eV have the spectroscopic factors of 0.006 and 0.002 and correspond to the ionization spectra of the terminal and central Mg atoms, respectively. The intense satellites at 1.85 and 2.76 eV ($\chi_c=0.11,0.079$) correspond to the ionization spectrum of the terminal Mg atoms and the satellite at 2.78 eV ($\chi_c=0.08$) to that of the central Mg atom. There is also a weak satellite ($\chi_c=0.008$) at 2.1 eV which is due to the ionization of the terminal Mg atoms.

TABLE VIII. Orbital energies (ε_i), GF ADC(4) ionization energies (E_i) and intensities ($\chi_c^{(i)}$) of the main lines in the Mg $2s^{-1}$ spectra of atomic Mg and Mg_n clusters. All energies in eV. Only nondegenerate states (splitting $\geqslant$0.001 eV) are listed.

Cluster	$-\varepsilon_i$	E_i	$\chi_c^{(i)}$	Comments
Mg	102.48	99.40(97.45)	0.785(0.787)	
Mg_2	102.47	98.87(96.94)	0.638(0.653)	
Mg_3 triangular	102.53	97.98	0.512	
Mg_3 linear	102.45	98.45	0.599	Central atom
	102.45	98.53	0.536	Terminal atoms
Mg_4 tetrahedral	102.51	97.92	0.551	
Mg_4 square	102.48	99.01	0.487	
Mg_4 linear	102.47	98.98	0.525	Internal atoms
	102.43	99.06	0.402	Terminal atoms

As seen in Table VIII, the splitting between the two lowest-energy states (main lines) of the linear Mg_4 cluster is very small (0.08 eV), like that of the linear Mg_3 cluster. The lowest-energy state corresponds to the ionization of the internal Mg atoms and the second main state is due to the ionization of the terminal ones. The spectroscopic factors of these two states are 0.525 and 0.402, respectively. The difference in the intensities can be attributed to a charge transfer from the external to the internal atoms upon the ionization of the terminal ones. This charge transfer is of an antiscreening type in contrast to the case of Be_4 where the charge transfer accompanying ionization of the terminal atoms is of a screening type. Thus, the effects due to the inequivalence of the atoms on the core-ionization spectrum of linear Mg_4 are similar to those in linear Be_3 rather than to those in linear Be_4. As can be seen in Table VII and VIII, the similarity of the processes accompanying ionization in the linear Be_3 and Mg_4 clusters is also reflected in the intensities of the split main lines in the spectra.

The first two weak satellites in the spectrum of linear Mg_4 appear at 0.88 and 1.02 eV and possess the spectroscopic factors $\chi_c = 0.015$ and 0.003, respectively. These satellites correspond to the ionization of the terminal and internal atoms, respectively. In contrast to the spectrum of linear Be_4, where there are only two relatively intense satellites in the energy interval up to ~ 3 eV above the lowest-energy state, the Mg $2s^{-1}$ spectrum of the linear Mg_4 cluster exhibits nine appreciably intense satellites in the same energy interval.

IV. DISCUSSION

Let us begin our discussion with the core-ionization of the dimers. Our analysis in terms of localized configurations shows that the low-lying intense satellites in the Be $1s^{-1}$ and Mg $2s^{-1}$ spectra of Be_2 and Mg_2 are dominated by the $l(rl)$ and $l(rr)$ configurations that are of interatomic character (Sec. III A). The $l(rl)$ configuration describes a transfer of a valence electron from the right atom to the left one, where the core hole has been created (see upper right panel of Fig. 4). Obviously, this excitation describes a *charge transfer* (CT). Furthermore, because the electron is transferred to the core-ionized site, this transferred charge *screens* the core hole. The $l(lr)$ configuration also represents a CT process, but in this case the electron is transferred from the core-ionized atomic site to the neutral neighboring atom. This CT, shown in the lower left panel of Fig. 4, is, consequently, of an *antiscreening* type. The $l(rr)$ configuration describes an interesting process where the creation of the core hole on one site is accompanied by a valence excitation of the neighboring neutral atom (upper left panel of Fig. 4). This process can be viewed as an *energy transfer* (ET) from the ionized atom to the neighboring one occurring upon ionization. Finally, the $l(ll)$ configuration depicted in lower right panel of Fig. 4 is a local valence excitation at that atomic site which has been core ionized.

In the spectrum of Be_2 the intense satellites at 1.68 and 4.47 eV are strong mixtures of the CT *screening* (CTS) and ET configurations (Table III). In contrast to Be_2, in the spectrum of Mg_2 the CT *screening* and ET features are well separated (Table IV). The satellites at 1.32 and 2.27 eV are mostly due to CTS whereas the satellites at 3.77 and 5.35 eV are dominated by the energy transfer configurations. Thus, the physical mechanisms responsible for the formation of the intense low-lying satellites in the spectra of Be_2 and Mg_2 govern the charge-transfer screening and energy transfer processes that are of interatomic (nonlocal) character.

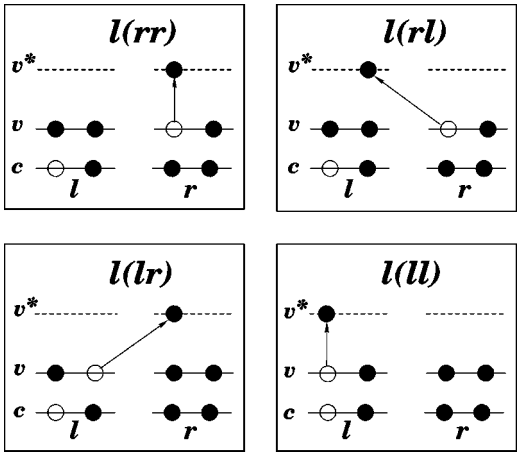

FIG. 4. Schematic representation of the basic intra-atomic and interatomic processes accompanying core ionization of weakly bound clusters. c, v, and v^* denote the core orbital, occupied valence orbitals, and unoccupied orbitals, respectively. l stands for one (say left) atom and r for the other (right) atom of the cluster.

It is worthwhile to analyze the spectra of the dimers in the limit of infinitely separated atoms (dissociation limit) where the interatomic interaction is negligible. In this case, of course, the spectral band shapes of the dimers are just exact replicas of the respective atomic spectra. There are, however, satellite states that correspond to interatomic processes and that are dark in spectra due to the negligible interatomic interaction. The computed $l^3(rl)$ and $l^1(rl)$ CTS states, for instance, appear in the spectrum of Be_2 (in the dissociation limit) at -0.09 and 1.17 eV, respectively. The corresponding CTS configurations can also be viewed as the $1s \rightarrow 2p$ core excitations of one Be atom and the simultaneous valence ionization of the other one. This point of view and the knowledge of the involved atomic energies allows one, in principle, to predict whether low-lying CTS shake-up or ever shake-down satellites are expected to appear in the spectra of a particular cluster. As long as the interatomic (intermolecular in the cases of molecular clusters) interaction is weak allowing the atoms constituting the cluster to largely keep their atomic character, the involved energies will usually, not change dramatically, but the interatomic satellites will acquire intensity and appear in the spectrum.

The energy of a CTS satellite at the dissociation limit is equal to the energy of the core-excited state of the atom plus the valence ionization energy of the neighboring atom. The relevant experimental atomic energies of Be are available in the literature. Using the Be $1s \rightarrow 2p$ core excitation energies of 114.3 eV (triplet state) and 115.4 eV (singlet state) [35], and the ionization energy of the Be $2s$ atomic shell of 9.32 eV [36], we find that the energies of the $l^3(rl)$ and $l^1(rl)$ satellites relative to the Be $1s^{-1}$ ionization energy of 123.6

eV [32] of the Be atom to be 0.02 and 1.12 eV, respectively. These values are very close to those calculated by the ADC(4) method and mentioned above (−0.09 and 1.17 eV, respectively). In contrast to Be_2 the CTS $l^3(rl)$ and $l^1(rl)$ satellites in Mg $2s^{-1}$ spectrum of Mg_2 appear in the dissociation limit according to our calculation at higher energies, namely, at 1.33 and 1.52 eV, respectively. The experimental Mg $2s \rightarrow 3p$ core-excitation energy is not reported in the literature and we cannot compare the computed satellite energies with experimental energies for singlet and triplet $l(rl)$ satellites in the case of Mg_2.

In the dissociation limit the computed ET $l^3(rr)$ and $l^1(rr)$ satellites appear in the spectrum of Be_2 at 3.04 and 6.09 eV and in the spectrum of Mg_2 at 2.50 and 4.51 eV, respectively. These ET configurations correspond to the triplet and singlet $2s \rightarrow 2p$ and $3s \rightarrow 3p$ excitations of the Be and Mg atoms infinitely separated from their counterpart that carries the core hole. The corresponding experimental energies of the $2s \rightarrow 2p$ triplet and singlet excitations in the Be atom are 2.725 and 5.277 eV, respectively [36]. For the Mg atom the energies of the triplet and singlet $3s \rightarrow 3p$ excitations are 2.709 and 4.345 eV, respectively [36]. We see that the energies of ET satellites in a cluster spectrum relative to the main line can be estimated by the energies of the valence excitations of those neutral atoms neighboring the atom where the core-hole has been created.

The $l(lr)$ CT antiscreening configurations negligibly contribute to the low-lying satellites of the dimers at reasonable interatomic distances. These configurations represent a rather exotic process: the core ionization of one of the atoms is accompanied by the valence excitation from the same atom to the other atomic center. In the dissociation limit the energy of such a process is the sum of the energy of the dication (valence ionized ion with the core hole) and that of the atomic negative ion. We have estimated the energy of the lowest of these states to be ~19 eV above the $2s^{-1}$ main state for Mg_2 and ~24 eV above the $1s^{-1}$ state for Be_2. Thus, it is clear that in the low-lying satellites these configurations do not admix with the other ones discussed above because of their high energy. The free atomic Mg^- and Be^- negative ions are not bound. However, at finite interatomic distances the energy of the $l(lr)$ antiscreening configuration can be substantially lower due to the stabilizing Coulomb interaction with the neighboring doubly positive ion. For example, the energy lowering of the Mg^- anion due to the Coulomb interaction with the dication Mg^{++} at the Mg-Mg equilibrium distance of 8 a.u. is as large as ~7 eV and the corresponding value for the Be^- anion at the Be-Be equilibrium distance of 5 a.u. is ~11 eV.

We arrive at the following overall picture of core ionization of small atomic clusters. The creation of a core hole is accompanied by different valence excitations. Due to the weak interaction between the atoms of the cluster, these excitations have distinct interatomic and intra-atomic characters. These processes are energetically well separated and the features corresponding to them are clearly identified in the core ionization spectra. The first low-lying intense satellites are mostly due to charge transfer from the neighboring atom. This CT is of the screening type. The intense satellites at slightly higher energies are due to energy transfer. These two types of interatomic processes are mostly responsible for the appearance of the unusually intense low-lying satellites in the core ionization spectra of the clusters. The intra-atomic features corresponding to the atomic dark states are very weak in the cluster spectra. We stress that in typical molecules (e.g., CO, N_2) one cannot distinguish between intra-atomic and interatomic processes accompanying ionization of core levels. This is due to the strong interaction (chemical bond) between the atoms that mixes all intra-atomic and interatomic excited configurations in all satellite states. Soft metal clusters provide an interesting class of objects with their own typical behavior (we have also studied some nonmetallic clusters and found related results). For these systems one can introduce the following classification of the satellites in the core ionization spectra (Fig. 5). All shake-up satellites are divided into two types: intra-atomic shake up and interatomic shake up. Interatomic shake-up satellites, in turn, are divided into ET and CT satellites. And finally, the CT shake-up satellites can be of the screening and antiscreening types. Some mixing among these contributions is, of course, possible. This classification is specific for weakly bound clusters only and is generally meaningless for typical molecules. Here, we should also note that in CO and N_2 molecules the first shake-up satellites appear at 8–10 eV above the main line and these satellites are very weak in contrast to the case of the atomic clusters studied in the present work.

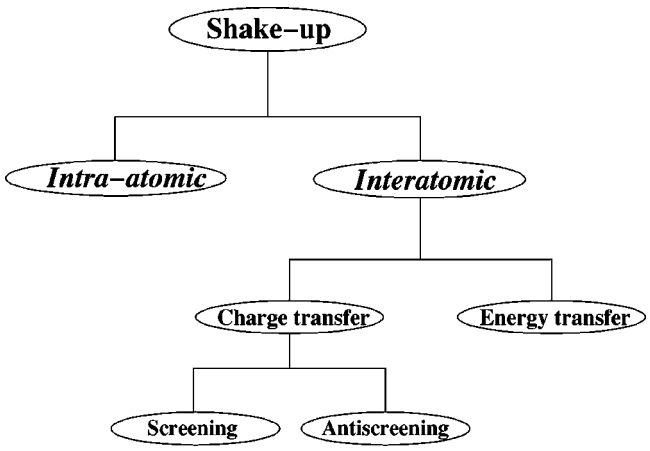

FIG. 5. The hierarchy of shake-up processes in the core ionization spectra of weakly bound clusters.

It is seen from Figs. 2 and 3 that the spectral band shapes of the clusters of different size and of different conformation appreciably different from each other. Several factors are responsible for this. First, the more atoms the more excitation channels are available in the presence of the core hole. Second, the number of the excitation channels, efficiently contributing to the spectral band shape, depends on the symmetry of the cluster. Third, the couplings of different excitation channels to each other and to the core hole depend on the interatomic distance. The latter results in the dependence of the spectral intensity distribution on the interatomic distance. The fact that the spectral band shapes are sensitive to the cluster size and conformation may be useful for the experimental spectral identification of clusters of a specific size and

conformation. In case there are atoms inequivalent due to symmetry (linear clusters in our study), a splitting of the main lines is observed. In the case of Mg_3 and Mg_4 the splitting is very small ($\sim$0.001 and $\sim$0.04 eV, respectively) in contrast to that in Be_3 and Be_4 which is considerable ($\sim$0.11 and $\sim$0.57 eV, respectively). Interestingly, splittings of the same magnitude are experimentally observed in the Be $1s^{-1}$ ionization spectrum of Be metal surfaces. The observations for the Be (0001) surface are 0.87, 0.605, 0.335, and 0.16 eV [37] and for Be$(10\bar{1}0)$ 0.7, 0.5, and 0.22 eV [38].

It is worthwhile to compare the dependence of the orbital energies on the size and conformation of the clusters with that of the ionization energies. Generally speaking, the difference between the core orbital energies of different clusters reflects the difference in their chemical bonding. In core-level spectroscopy such a change of core-ionization energy is referred to as the chemical shift. The difference between the orbital energies of the Be atom and Be_2 cluster is very small ($\sim$0.02 eV) whereas the respective ionization energies differ substantially by 2.08 eV. This means that the chemical bonding plays a minor role in lowering the ionization energy of Be_2 with respect to the Be atom. This lowering is essentially only due to relaxation and correlation in the final core-ionized states of the Be_2 cluster. When increasing the cluster size, the contribution of the chemical bonding to the ionization energy lowering becomes larger: the difference between the core orbital energies of the Be_2 dimer and the Be_3 triangular cluster is 0.27 eV and that between the ionization energies is 1.29 eV. The difference between the orbital energies of the Be_3 triangular and Be_4 tetrahedral clusters is 0.74 eV. This value is close to the respective difference between the ionization energies (0.96 eV). In the linear Be_3 cluster the orbital energy splitting due to the inequivalence of atoms is 0.11 eV. The respective splitting of the ionization energies is 0.31 eV. Also, this splitting is seen to be sensitive to electron relaxation and electron correlation. Surprisingly, the situation is different in the linear Be_4 cluster where the splittings between the orbital energies of the terminal and central atoms and that of the respective ionization energies are very close to each other: 0.57 and 0.62 eV, respectively.

One observes a similar behavior for the Mg clusters (Table VIII). There seems to be a kind of saturation of the many-body contributions to the lowering of the first core ionization energy in the clusters: for small clusters (Be_2, triangular Be_3, Mg_2, triangular Mg_3) the major contribution to the ionization energy lowering is due to many-body effects; from some size on (Be_4,Mg_4 tetrahedral) the major contribution to the energy lowering is due to changes in the chemical bonding. It could be that the shortening of the prevailing intermolecular distances also plays a role in this behavior.

V. MAIN CONCLUSIONS

Our GF ADC(4) calculations on small Mg and Be clusters have revealed remarkable cluster-specific features in their core ionization spectra. These intense features have distinct *interatomic* character and can be experimentally detected. Charge transfer and energy transfer processes have been shown to be responsible for the appearance of these intense low-lying satellites. The spectra are sensitive to the size and conformation of the clusters. This can be used for the experimental identification of the clusters. The resulting physical picture of the core ionization of small atomic metal clusters is transparent and can be expected to apply to weakly bound molecular clusters as well. The intensities and energies of the low-lying satellites in other systems will, of course, depend on the specific properties of the corresponding molecules. Of particular importance in the investigation of cluster spectra is that by a proper choice of clusters one can separately study different physical processes such as energy transfer and charge transfer between the monomers in the cluster.

ACKNOWLEDGEMENTS

Valuable discussions with J. Schirmer are gratefully acknowledged. Financial support by the DFG is acknowledged.

[1] *Clusters of Atoms and Molecules I*, edited by H. Haberland, Springer Series in Chemical Physics (Springer, Berlin, 1994), Vol. 52.
[2] J. Michl, Chem. Rev. **94**, 7 (1994).
[3] K. Lin, J. D. Cruzan, and R. J. Saykally, Science **272**, 929 (1996).
[4] *The Chemical Physics of Atomic and Molecular Clusters*, edited by G. Scoles (North-Holland, Amsterdam, 1990).
[5] W. A. de Heer, Rev. Mod. Phys. **65**, 611 (1993).
[6] V. Bonačič-Koutecký, P. Fantucci, and J. Kontecký, Chem. Rev. **91**, 1035 (1991).
[7] O. Björneholm, F. Federmann, F. Fössing, and T. Möller, Phys. Rev. Lett. **74**, 3017 (1995).
[8] O. Björneholm, F. Federmann, F. Fössing, and T. Möller, J. Chem. Phys. **104**, 1846 (1996).
[9] E. Rühl, A. Knop, D. N. Mcllroy, Surf. Rev. Lett. **3**, 557 (1996).
[10] O. Björneholm, F. Federmann, S. Kakar, and T. Möller, J. Chem. Phys. **111**, 546 (1999).
[11] L. S. Cederbaum, J. Zobeley, and F. Tarantelli, Phys. Rev. Lett. **79**, 4778 (1997).
[12] J. Zobeley, L. S. Cederbaum, and F. Tarantelli, J. Chem. Phys. **108**, 9737 (1998).
[13] R. Santra, J. Zobeley, L. S. Cederbaum, and N. Moiseyev, Phys. Rev. Lett. **85**, 4490 (2000).
[14] W. Klopper and J. Almlöf, J. Chem. Phys. **99**, 5167 (1993).
[15] V. E. Bondybey, Chem. Phys. Lett. **109**, 436 (1984).
[16] W. J. Balfour and A. E. Douglas, Can. J. Phys. **48**, 901 (1970); C. R. Vidal and H. Scheingraber, J. Mol. Spectrosc. **65**, 46 (1977).
[17] J. Schirmer, L. S. Cederbaum, and O. Walter, Phys. Rev. A **28**, 1237 (1983).
[18] G. Angonoa, O. Walter, and J. Schirmer, J. Chem. Phys. **87**, 6789 (1987).

[19] L. S. Cederbaum, W. Domcke, J. Schirmer, and W. von Niessen, Adv. Chem. Phys. **65**, 115 (1986).
[20] W. Domcke, L. S. Cederbaum, J. Schirmer, and W. von Niessen, Phys. Rev. Lett. **42**, 1237 (1979).
[21] N. V. Dobrodey, L. S. Cederbaum, and F. Tarantelli, Phys. Rev. B **57**, 7340 (1998).
[22] M. W. Schmidt *et al.*, J. Comput. Chem. **14**, 1347 (1993).
[23] R. Krishnan, J. S. Binkley, R. Seeger, J. A. Pople, J. Chem. Phys. **72**, 650 (1980).
[24] GAUSSIAN98, Revision A.7, Gaussian, Inc., Pittsburgh, PA, 1998.
[25] I. G. Kaplan, S. Roszak, and J. Leszczynski, J. Chem. Phys. **113**, 6245 (2000).
[26] P. V. Sudhakar and K. Lamertsma, J. Chem. Phys. **99**, 7929 (1993).
[27] T. J. Lee, A. P. Rendell, and P. R. Taylor, J. Chem. Phys. **92**, 489 (1990).
[28] M. M. Marino and W. C. Ermler, J. Chem. Phys. **86**, 6283 (1987).
[29] H. Partrige, C. W. Bauschlicher, Jr., L. G. M. Petterson, Jr., A. D. Mclean, B. Lin, M. Yoshimine, and A. Komornicki, J. Chem. Phys. **92**, 5377 (1990).
[30] M. S. Banna, B. Wallbank, D. C. Frost, C. A. McDowell, and J. S. H. Q. Perera, J. Chem. Phys. **68**, 5459 (1978).
[31] B. Breuckmann, V. Schmidt, and W. Schmidtz, J. Phys. B **9**, 3037 (1976).
[32] M. Rødbro, R. Bruch, and P. Bisgaard, J. Phys. B **12**, 2413 (1979).
[33] G. De Alti, P. Decleva, and A. Lisini, Chem. Phys. **93**, 225 (1985).
[34] N. V. Dobrodey, L. S. Cederbaum, and F. Tarantelli, Phys. Rev. B **61**, 7336 (2000).
[35] M. O. Krause and C. D. Caldwell, Phys. Rev. Lett. **59**, 2736 (1987).
[36] S. Bashkin and J. O. Stoner, Jr., *Atomic Energy Levels and Grotrian Diagrams* (North-Holland/American Elsevier, Amsterdam/New York, 1975), Vol. I.
[37] L. I. Johansson, P.-A. Glans, and T. Balasubramanian, Phys. Rev. B **58**, 3621 (1998).
[38] S. Lizzit, K. Pohl, A. Baraldi, G. Comelli, V. Fritzsche, E. W. Plummer, R. Stumpf, and Ph. Hoffmann, Phys. Rev. Lett. **81**, 3271 (1998).